arXiv:0705.2866v1 [cond-mat.mtrl-sci] 20 May 2007

Electromagnetic wave propagation in an almost circular bundle of closely packed, metallic, carbon nanotubes

M. V. Shuba, S. A. Maksimenko
Institute for Nuclear Problems, Belarus State University, Bobruiskaya 11, 220050 Minsk, Belarus

A. Lakhtakia
Department of Engineering Science and Mechanics, Pennsylvania State University, University Park, PA 16802-6812, USA

An equivalent-multishell approach for the approximate calculation of the characteristics of electromagnetic waves propagating in almost circular (azimuthally symmetric), closely packed bundles of parallel, identical, and metallic carbon nanotubes (CNTs) yields results in reasonably good agreement with a many-body technique, for infinitely long bundles when the number of CNTs is moderately high. The slow-wave coefficients for azimunthally symmetric guided waves increase with the number of metallic CNTs in the bundle, tending for thick bundles to unity, which is characteristic of macroscopic metallic wires. The existence of an azimuthally nonsymmetric guided wave at low frequencies in a bundle of a large number of finite-length CNTs stands in contrast to the characteristics of guided-wave propagation in a single CNT. The equivalent-multishell approach yields the polarizability scalar and the antenna efficiency of a bundle of finite-length CNTs in the long-wavelength regime over a wide frequency range spanning the terahertz and the near-infrared regimes. Edge effects give rise to geometric resonances in such bundles. The antenna efficiency of a CNT bundle at the first resonance can exceed that of a single CNT by four orders of magnitude, which is promising for the design and development of CNT-bundle antennas and composite materials containing CNT-bundles as inclusions.

PACS numbers: 42.70.-a, 73.25.+i, 77.84.Lf, 78.67.Ch

I. INTRODUCTION

Carbon nanotubes (CNTs) have been the subjects of intensive research in the area of nanotechnology for about 15 years [1], yet understanding of their fundamental physics is far from complete. One topic under intensive investigation is their electromagnetic response. Early theoretical studies on CNTs, modeled as infinitely long cylinders of a gas of electrons, showed the existence of gapless, low-frequency, plasmon branches [2]. The low-frequency plasmon excitation along the nanotube axis lead to the formation of a electromagnetic surface wave [3]. This surface wave strongly influences the scattering [4] and radiation [5, 6] properties of a CNT in the terahertz regime.

Guided-wave propagation should therefore occur in a CNT bundle containing $2 \sim 1000$ parallel CNTs closely packed together. A guided wave could be formed by the plasmonic excitation in every CNT in the bundle and its characteristics would strongly depend on interactions between the CNTs. Two types of such interactions have been discussed in the literature:

(i) The first type of interaction arises from the direct coupling of the electronic states in adjacent CNTs due to overlap of their electron wavefunctions [7]. The overlap is always very small for two reasons: (a) the contact area between two adjacent CNTs is small due to their geometric curvature, even when the two touch each other; and (b) the orbitals of the carbon atoms strongly overlap only in the plane of a graphene sheet, which leads to the known van der Waals form of the integraphene sheet interaction. The momentum mismatch between the Fermi points of neighboring CNTs suppresses the inter-CNT tunneling and leads to strong localization of electronic eigenstates on individual CNTs. Therefore, there is no significant change of low-energy band structure in the vicinity of the Fermi energy of a compositionally disordered metallic CNT bundle [7] as compared with band structure of a single CNT.

(ii) The second type of interaction is an electrodynamic coupling in which Coulomb interactions in a CNT are modified by the dielectric screening induced by the adjacent CNTs. Such dielectric screening has a significant effect in 1D structures (such as single-wall CNTs) since many-body interactions are intrinsically strong in 1D geometry because much of the electric field of a charge on a CNT extends outside of the CNT.

A bundle of parallel CNTs is generally considered as a 2D array of infinitely long CNTs [8, 9, 10], thereby allowing the determination of the dispersion properties of a low-frequency plasmon in a 2D periodic medium. A realistic bundle of almost circular cross-section has a cross-sectional diameter much less than both its length and the electromagnetic wavelength in free space. In order to determine the scattering and radiation properties of a realistic CNT bundle, one needs to consider both the finite diameter and the length of the bundle.

Our aim in this paper is to analyze guided-wave propagation in an almost circular bundle of metallic CNTs all of which are either infinitely long or have finite length. We neglect modifications of the low-energy band structure of

CNTs, but not the electromagnetic coupling of CNTs in a bundle. Following Selpyan *et al.* [3], we assume that, in the low-frequency regime below optical interband transitions, the conductivity of metalic CNTs is described by the electron-gas model, thereby leading to the CNT conductivity to follow the Drude model.

The rest of this paper is organized as follows. In Secs. II and III, a many-body technique and an equivalent-multishell approach, respectively, are applied to a bundle of infinitely long metallic CNTs to derive dispersion equations for guided-wave propagation on the bundle. In Sec. IV, scattering theory is applied to a bundle of finite-length CNTs. Sec. V contains numerical results for guided-wave parameters obtained from different approaches.

II. GUIDED WAVES IN A BUNDLE OF INFINITELY LONG CNTS

A. Many-body technique

Let us examine the propagation of a guided wave in an isolated bundle of N metallic CNTs that are closely packed together and are of infinite length. The surrounding medium is free space (i.e., vacuum). The effective cross-sectional diameter of the bundle is much smaller than the wavelength in free space, and the transverse current in all CNTs in the bundle is neglected. An $\exp(-i\omega t)$ time-dependence is implicit, with $i = \sqrt{-1}$, t denotes the time, and ω is the angular frequency.

In the low-frequency regime, only intraband transitions of π-electrons with unchanged transverse quasi-momentum are allowed [11]. These transitions contribute to the axial conductivity, but not to the transverse conductivity [12], and excite azimuthally symmetric electric current densities in the CNTs [3, 13]. At frequencies far away from interband resonances, in practical terms, azimuthally nonsymmetric electric current densities are not excited in CNTs because the relevant conductivities vanish. In detail, this peculiarity has been discussed elsewhere [2, 14] with application to surface-plasmon modes. In the remainder of this paper, therefore we restrict ourselves to azimuthally symmetric electric current densities in the CNTs forming the bundle.

The superposition of the fields, induced by the electric current densities on the surfaces of all CNTs together form a guided wave in the CNT bundle. The electric Hertz vector $\mathbf{\Pi}_m(\mathbf{r}) \equiv \Pi_m(\mathbf{r})\mathbf{e}_z$ created by the axial electric current density on the surface of the mth CNT ($m \in [1, N]$) in the bundle is governed by the Helmholtz equation

$$(\nabla^2 + k^2)\mathbf{\Pi}_m(\mathbf{r}) = \mathbf{0}\,, \tag{1}$$

where $\mathbf{e}_z$ is the unit vector along the CNT axis (and therefore the axis of the bundle), $k = \omega/c$, and c is speed of light in vacuum. Let the origin of the cylindrical coordinate system $(\rho^{(m)}, \phi^{(m)}, z)$ be located at the point $z = 0$ on the axis of the mth CNT. Since Π_m is a function only of $\rho^{(m)}$ and z for an azimuthally symmetric electric current density, the nonzero components of the electromagnetic field in this cylindrical coordinate system are as follows:

$$E^m_{\rho^{(m)}} = \frac{\partial^2 \Pi_m}{\partial \rho^{(m)} \partial z}\,, \tag{2}$$

$$E^m_z = \Big(\frac{\partial^2}{\partial z^2} + k^2\Big)\Pi_m\,, \tag{3}$$

$$H^m_{\phi^{(m)}} = ik\frac{\partial \Pi_m}{\partial \rho^{(m)}}\,. \tag{4}$$

The electric Hertz potential Π_m must satisfy the effective boundary conditions [3]

$$\frac{\partial \Pi_m}{\partial \rho^{(m)}}\bigg|_{\rho^{(m)}=R_m+0} - \frac{\partial \Pi_m}{\partial \rho^{(m)}}\bigg|_{\rho^{(m)}=R_m-0} = \frac{4\pi\sigma_m}{ikc}\left[\frac{\partial^2 \Pi_m}{\partial z^2} + k^2\Pi_m + E^{m0}_z + \sum_{s=1, s\neq m}^{N} E^{ms}_z(z)\right]\,, \tag{5}$$

$$\Pi_m\Big|_{\rho^{(m)}=R_m+0} = \Pi_m\Big|_{\rho^{(m)}=R_m-0}\,, \tag{6}$$

where σ_m is the axial conductivity of the mth CNT in isolation. The scalar fields $E^{m0}_z(z)$ and $E^{ms}_z(z)$ are the z-directed components of the electric field on the surface of the mth CNT, produced by the externally impressed sources and the axial current density on the sth CNT, respectively.

Below the frequency regime of optical transitions, an expression for the axial conductivity σ_m is available via quantum transport theory as [3]

$$\sigma_m(\omega) = -\frac{ie^2}{\pi^2\hbar R_m}\frac{1}{(\omega + i/\tau)}\sum_{n=1}^{\tilde{m}}\int\limits_{1stBZ}\frac{\partial F_c}{\partial p_z}\frac{\partial \mathcal{E}_c}{\partial p_z}dp_z\,, \tag{7}$$

where e is the electron charge, $\hbar$ is the normalized Planck constant, and p_z is the axial projection of the electron quasi–momentum. The integer $n \in [1, \tilde{m}]$ labels the π-electron energy bands, with $\tilde{m}$ appearing in the dual index $(\tilde{m}, \tilde{n})$ used to classify CNTs [11]. The time constant τ of the electron mean-free-path is assumed to be equal to the inverse relaxation frequency. The abbreviation $1stBZ$ restricts the variable p_z to the first Brillouin zone. The equilibrium Fermi distribution function

$$F_c(p_z, n) = \frac{1}{1 + \exp\left[\dfrac{\mathcal{E}_c(p_z, n)}{k_B T}\right]} \tag{8}$$

involves the temperature T and the Boltzmann constant k_B. The electron energy $\mathcal{E}_c(p_z, n)$ for zigzag $(\tilde{m}, 0)$ CNTs is [11]

$$\mathcal{E}_c = \gamma_0\sqrt{1 + 4\cos\left(ap_z\right)\cos\left(\frac{\pi n}{\tilde{m}}\right) + 4\cos^2\left(\frac{\pi n}{\tilde{m}}\right)}\,; \tag{9}$$

where $\gamma_0 \approx 2.7$ eV is the overlapping integral [11], $a = 3b/2\hbar$, and $b = 0.142$ nm is the interatomic distance in graphene. An expression for $\mathcal{E}_c(p_z, n)$ for armchair $(\tilde{m}, \tilde{m})$ CNTs is also available [11].

B. Dispersion equation

A solution of Eq. (1) that satisfies the boundary condition (6) is as follows:

$$\Pi_m(\rho^{(m)}, z) = \\ A_m e^{ihz}\begin{cases} K_0(\kappa R_m)I_0(\kappa\rho^{(m)}), & \rho^{(m)} < R_m \\ I_0(\kappa R_m)K_0(\kappa\rho^{(m)}), & \rho^{(m)} > R_m \end{cases}. \tag{10}$$

Here A_m is an amplitude, h is the guide wavenumber to be determined, and $\kappa = \sqrt{h^2 - k^2}$, while $I_0(\cdot)$ and $K_0(\cdot)$ are the modified Bessel functions of order 0. Equation (5) still has to be satisfied.

The field $E_z^{ms}(z)$ in Eq. (5) may be found by applying Eqs. (3) and (10) in the coordinate system $(\rho^{(s)}, \phi^{(s)}, z)$ to the sth CNT, $s \neq m$, and then using the addition theorem for $K_0(\kappa\rho^{(s)})$, $\rho^{(s)} > R_s$, to translate to the coordinate system $(\rho^{(m)}, \phi^{(m)}, z)$ [15]. With $\rho^{(s)}$ lying on the surface of the mth CNT, as shown in Fig. 1(a), we get

$$E_z^{ms}(\rho^{(s)}, z) = -A_s\kappa^2 e^{ihz}I_0(\kappa R_s)K_0(\kappa\rho^{(s)}) = \\ -A_s\kappa^2 e^{ihz}I_0(\kappa R_s)\sum_{\ell=-\infty}^{\infty}K_\ell(\kappa d_{sm})I_\ell(\kappa R_m)e^{i\ell\phi^{(m)}}\,, \tag{11}$$

where d_{sm} is the distance between the axes of the two CNTs and the angle $\phi^{(m)}$ has been identified in Fig. 1(a).

As the conductivities for azimuthally nonsymmetric modes ($\ell \neq 0$) are assumed to be null-valued, only the $\ell = 0$ term in Eqs. (11) survives after the substitution that equation into Eq. (5). Thereafter, the substitution of Eqs. (10) and (11) into Eq. (5) with $E_z^{m0}(z) = 0$ and the subsequent use of the Wronskian of modified Bessel functions [15] lead to the following set of linear homogeneous equations with unknown A_s, $s \in [1, N]$, written in the matrix form as

$$\mathsf{MA} = 0\,. \tag{12}$$

Here, A is a column vector containing the N unknowns A_s, and the element M_{sm} of the $N \times N$ matrix M is given by

$$M_{sm} = \begin{cases} K_0(\kappa d_{sm})I_0(\kappa R_m), & s \neq m, \\ K_0(\kappa R_s) - i\omega/[4\pi R_s\sigma_s\kappa^2 I_0(\kappa R_s)], & s = m. \end{cases}$$

The set (12) of linear equations has nontrivial solutions provided

$$\det\mathsf{M} = 0\,. \tag{13}$$

The dispersion equation (13) has N roots corresponding to N guided waves in the CNT bundle. The solution of Eq. 13 allows us to obtain the slow-wave coefficients $\beta = k/h$ of guided waves in the CNT bundle.

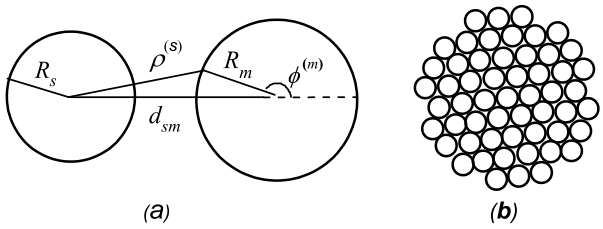

FIG. 1: (a) Schematic of two CNTs in a bundle to identify various quantities appearing in Eq. (11). (b) A bundle of $N = 55$ closely packed CNTs that can be approximately taken to have azimuthal symmetry, and thus has an almost circular cross-section.

III. EQUIVALENT-MULTISHELL APPROACH

The many-body technique is cumbersome for a CNT bundle with large N. Furthermore, we are interested in guided waves with azimuthal symmetry, corresponding to the low-h roots of Eq. (13), as such waves are easily excited in bundles by uniform external fields, and are also relevant for bundles of finite-length CNTs in the long-wavelength regime (Sec. IV).

An approximate but simpler method for low-h guided waves can be devised for an almost circular bundle of closely packed and *identical* CNTs as follows. Let R_b stand for an effective cross-sectional radius of the bundle. Since the electromagnetic field of the guided wave is azimuthally symmetric both inside and outside the bundle, we can model the bundle as a multishell structure comprising $\tilde{N}$ concentric shells. Each shell in this equivalent-multishell structure is infinitesimally thin. Thus, the pth shell, $p \in [1, \tilde{N}]$, has a cross-sectional radius $\tilde{R}_p$ such that $R_b = \tilde{R}_{\tilde{N}} > \tilde{R}_{\tilde{N}-1} > ... > \tilde{R}_1$. The effective surface conductivity of the pth shell is given by $\tilde{\sigma}_p = \Sigma_p/(2\pi\tilde{R}_p)$, where Σ_p is equal to the sum of the axial conductivities of all CNTs placed between the pth and the (p$-$1)th shells. There is some latitude inherent in the procedure to select $\tilde{N}$, $\tilde{R}_p$, and $\tilde{\sigma}_p$, $p \in [1, \tilde{N}]$.

Let $\Pi_p(\rho, \phi, z)$ be the Hertz potential everywhere *entirely* due to the pth shell, with the cylindrical coordinate system (ρ, ϕ, z) located at the point $z = 0$ on the axis of the CNT bundle. The boundary conditions across the pth shell due to the axial current density $\mathbf{J}_p(z) = J_p(z)\mathbf{e}_z$ on the surface $\rho = \tilde{R}_p$ are as follows:

$$\left.\frac{\partial \Pi_p}{\partial \rho}\right|_{\rho=\tilde{R}_p+0} - \left.\frac{\partial \Pi_p}{\partial \rho}\right|_{\rho=\tilde{R}_p-0} = \frac{4\pi}{ikc} J_p \,, \tag{14}$$

$$\left.\Pi_p\right|_{\rho=\tilde{R}_p+0} = \left.\Pi_p\right|_{\rho=\tilde{R}_p-0} . \tag{15}$$

Here

$$J_p(\phi, z) = \tilde{\sigma}_p \left[\sum_{q=1}^{\tilde{N}} \left[\frac{\partial^2}{\partial z^2} + k^2 \right] \Pi_q(\tilde{R}_p, \phi, z) + E_z^0(z) \right] , \tag{16}$$

where E_z^0 is the z-directed component of the externally impressed electric field.

With $A_p^{(\ell)}$, $\ell \in [0, \infty)$, representing its amplitude, an expression for Π_p is as follows:

$$\Pi_p(\rho, \phi, z) = A_p^{(\ell)} e^{ihz} e^{i\ell\phi} \begin{cases} K_\ell(\kappa\tilde{R}_p) I_\ell(\kappa\rho), & \rho < \tilde{R}_p, \\ I_\ell(\kappa\tilde{R}_p) K_\ell(\kappa\rho), & \rho > \tilde{R}_p. \end{cases} \tag{17}$$

Substitution of (16) with $E_z^0 = 0$ and Eqs. (17) into Eq. (14) leads to a set of linear homogeneous equations with unknown $A_p^{(\ell)}$, $p \in [1, \tilde{N}]$. This set has nontrivial solutions that can be ascertained by solving dispersion equation

$$\det \tilde{\mathsf{M}} = 0 \tag{18}$$

for the determination of h. The element $\tilde{M}_{qp}$ of the $\tilde{N} \times \tilde{N}$ matrix $\tilde{\mathsf{M}}$ is to be computed as

$$\tilde{M}_{qp} = \begin{cases} K_\ell(\kappa\tilde{R}_q) I_\ell(\kappa\tilde{R}_p), & q < p, \\ K_\ell(\kappa\tilde{R}_p) I_\ell(\kappa\tilde{R}_q), & q > p, \\ K_\ell(\kappa\tilde{R}_q) I_\ell(\kappa\tilde{R}_q) - i\omega/[4\pi\tilde{R}_q\tilde{\sigma}_q\kappa^2], & q = p. \end{cases}$$

For almost circular bundles with $N = 55$ CNTs, we compared the first three solutions of Eq. (13) with those of Eq. (18) for $\ell = 0$, and obtained good agreement, as discussed in Sec. V.

In contrast to an isolated CNT and even a bundle with relatively small number of closely packed CNTs, in the low-frequency regime an azimuthally nonsymmetric guided wave with $\ell \neq 0$ can exist in a CNT bundle with a large number of CNTs. This guided wave is formed by the ensemble of azimuthally symmetric electric current densities excited in every CNT of the bundle. The local field of the azimuthally nonsymmetric wave quickly changes in the central part of the bundle. Since symmetric electric current densities are excited by the spatially homogeneous component of the local field, then CNTs in the central core of the bundle practically are not excited and their conductivity may be supposed to be zero. Therefore, in order to approximately describe an azimuthally asymmetric guided wave by Eqs. (17) and (18), the conductivity of the inner shells with radius $\tilde{R}_p < 10\ell R_0/\pi$ should be assumed to be equal to zero, where R_0 is the radius of every CNT in the bundle. It is expected that an azimuthally nonsymmetric guided wave can be easily excited in a bundle of parallel closely placed CNTs and contribute greatly to interbundle interactions.

IV. GUIDED WAVES IN A BUNDLE OF FINITE-LENGTH CNTS

In order to investigate the finite-length effects in CNT bundles, let us apply integral-equation methods developed for a single CNT [4, 5] and for a planar array of CNTs [16, 17]. Let a closely packed bundle of parallel and identical CNTs of length L be aligned parallel to the z axis of a Cartesian coordinate system. The bundle has an almost circular cross-section so the bundle radius R_b can be prescribed; R_b is assumed here to be much less than the wavelength λ and length L. On exposure to an externally impressed field that is almost homogeneous over the bundle cross-section, an axial and azimuthally symmetric surface current density is excited in every CNT. Following Sec. III, we replace the CNT bundle by $\tilde{N}$ multishells, and prescribe the radius $\tilde{R}_p$ as well as the effective axial conductivity $\tilde{\sigma}_p$ of the p^{th} shell, $p \in [1, \tilde{N}]$. The surface current density, induced by the externally impressed field on the surface of the p^{th} shell, is denoted by $\mathbf{J}_p(z) = J_p(z)\mathbf{e}_z$. It has to satisfy the edge conditions

$$J_p(\pm L/2) = 0, \tag{19}$$

which express the absence of concentrated charges on the two edges of the bundle.

The electric Hertz potential $\Pi(\rho, z)$ satisfies the Helmholz equation (1), the radiation condition [18], as well as the the boundary conditions (14) and (15); the cylindrical coordinate system (ρ, ϕ, z) located at the point $z = 0$ on the axis of the CNT bundle. The potential $\Pi(\rho, z)$ is expressed in the form of a single-layer potential as

$$\Pi(\rho, z) = \frac{i}{\omega} \sum_{p=1}^{\tilde{N}} \tilde{R}_p \int_{-L/2}^{L/2} J_p(z') G(z - z', \rho, \tilde{R}_p) dz' , \tag{20}$$

where

$$G(z, \rho, R) = \int_0^{2\pi} \frac{\exp\left\{ik\sqrt{\rho^2 + R^2 - 2R\rho\cos\varphi + z^2}\right\}}{\sqrt{\rho^2 + R^2 - 2R\rho\cos\varphi + z^2}} d\varphi \tag{21}$$

is the free-space scalar Green function and

$$J_p(z) = \tilde{\sigma}_p \left[\frac{\partial^2 \Pi(\tilde{R}_p, z)}{\partial z^2} + k^2 \Pi(\tilde{R}_p, z) + E_z^0(z) \right]. \tag{22}$$

Setting $\rho = \tilde{R}_p$ in Eq. (20) and making use of Eq. (22), we obtain a system of $\tilde{N}$ integral equations with respect to the unknown current densities as follows:

$$\Phi_p(z) = \sum_{q=1}^{\tilde{N}} \int_{-L/2}^{L/2} \left\{ \frac{i2\pi\tilde{R}_q}{\omega} G(z - z', \tilde{R}_q, \tilde{R}_p) - \frac{\delta_{qp}}{2ik\tilde{\sigma}_q} \exp(ik|z - z'|) \right\} \times J_q(z') dz' , \quad p \in [1, \tilde{N}] . \tag{23}$$

Here,

$$\Phi_p(z) = -\frac{1}{2ik\tilde{\sigma}_p} \int_{-L/2}^{L/2} E_z^0(z') \exp(ik|z-z'|)dz'$$

$$+C_p \exp(ikz) + D_p \exp(-ikz) \tag{24}$$

and δ_{qp} is the Kronecker delta, whereas C_p and D_p are unknown constants to be determined from the edge conditions (19). Parenthetically, the system (23) with a different Green function was applied to a planar array of finite CNTs [16, 17].

The integral on the right side of (23) can be numerically handled by a quadrature formula, thereby transforming the system (23) into a matrix equation. The solution of the corresponding characteristic equation yields eigenfrequencies and eigenmodes of a finite coaxial cylinder as a high-Q microcavity.

In the long-wavelength regime ($\lambda \gg L$), the electromagnetic properties of the CNT bundle can be characterized by the polarizability scalar

$$\alpha = \frac{2\pi i}{\omega E_z^0(0)} \sum_{p=1}^{\tilde{N}} \tilde{R}_p \int_{-L/2}^{L/2} J_p(z)dz \tag{25}$$

As shown elsewhere [4, 5, 6], an isolated CNT can function as an antenna in the terahertz regime wherein the CNT has geometrical resonances of guided wave with slow-wave coefficient β_0 at frequencies related to the CNT length L by the condition

$$Lk \approx \pi \tilde{s}\, \mathrm{Re}(\beta_0), \quad \tilde{s} = 1, 2, \dots , \tag{26}$$

where β_0 is the slow-wave coefficient for an isolated CNT. The antenna effect of an array of multiwall CNTs was experimentally found at a frequency satisfying the condition (26) with $\tilde{s} = 1$ and $\beta_0 \approx 1$ [19, 20].

In this paper, we are interested in the antenna efficiency of a CNT bundle at the first antenna resonance: $\tilde{s} = 1$ in Eq. (26). The antenna efficiency is defined as the ratio

$$\eta = \frac{P_r}{P_t + P_r}, \tag{27}$$

where

$$P_r = \frac{\pi^2 \omega^2}{c^3} \int_0^{\pi} \sin^3\theta \left| \int_{-L/2}^{L/2} e^{ikz\cos\theta} \sum_{p=1}^{\tilde{N}} \tilde{R}_p J_p(z)dz \right|^2 d\theta \tag{28}$$

is the radiated power and

$$P_t = \pi \mathrm{Re} \left(\sum_{p=1}^{\tilde{N}} \frac{\tilde{R}_p}{\tilde{\sigma}_p} \int_{-L/2}^{L/2} |J_p(z)|^2 dz \right) \tag{29}$$

is the power lost to ohmic dissipation.

In the long-wavelength regime, the antenna efficiency η_0 of an isolated CNT is equivalent to that of a dipole antenna of length L and resistance per unit length R_{dip} [6]; i.e.,

$$\eta_0 = \frac{L/\lambda}{L/\lambda + 3cR_{dip}\lambda/(8\pi^2)}, \tag{30}$$

where $R_{dip} = \mathrm{Re}[1/(2\pi R_0 \sigma_0)]$ for an isolated CNT of cross-sectional radius R_0 and surface conductivity σ_0. The high value of R_{dip} [21] and the small value of L/λ at the first antenna resonance lead to a very small antenna efficiency of an isolated single CNT, i.e., $\eta_0 \approx 10^{-4} - 10^{-6}$ [5, 6].

However, the situation is more optimistic for a bundle of N metallic CNTs. Such a CNT bundle can be considered as a composite antenna containing N in-phase parallel dipole antennas, so that $P_r \sim N^2$ but $P_t \sim N$ from Eqs. (28)

and (29). Then the antenna efficiency of the CNT bundle at the frequency of first geometrical resonance of the axially symmetric guided wave with the highest slow-wave coefficient β is

$$\eta \approx \frac{N\eta_0 \,\mathrm{Re}(\beta)}{\eta_0[N\,\mathrm{Re}(\beta) - \mathrm{Re}(\beta_0)] + \mathrm{Re}(\beta_0)}, \tag{31}$$

where η_0 is the antenna efficiency of an isolated CNT at the first antenna resonance at the same frequency.

Because of electromagnetic coupling of the CNTs in a bundle with $N \gg 1$ CNTs, the inequality $\mathrm{Re}(\beta) \gg \mathrm{Re}(\beta_0)$ holds true, as shown in Sec. V; therefore, $\eta \gg \eta_0$.

V. CHARACTERISTICS OF GUIDED WAVES

Calculations were performed for almost circular bundles made of N parallel, identical, single-wall, metallic, zigzag (21,0) CNTs. The relaxation time was taken as $\tau = 10^{-13}$ s. For convenience, the CNTs were assumed to be close-packed on a 2D triangular lattice with intertube spacing 3.4 Å as shown in Fig. 1(b) for $N = 55$.

A. Guided waves in bundles of infinitely long CNTs

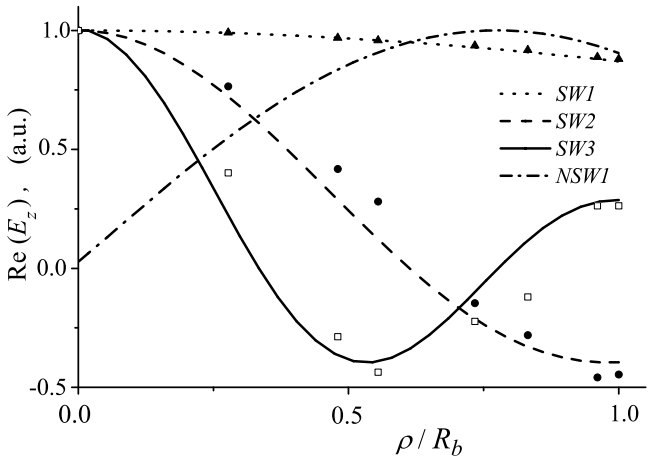

FIG. 2: Radial dependencies of the magnitude of the z-directed component of the electric field (in arbitrary units) of the guided waves in a CNT bundle of $N = 55$ parallel, identical, infinitely long, single-wall, metallic, zigzag (21,0) CNTs arranged on a triangular lattice. The points correspond to the solutions of Eq. (13), and the lines to the solutions of Eq. (18).

Let us begin with numerical results for bundles of infinitely long CNTs. We considered only three roots each of the dispersion equations (13) and (18). These roots — labeled h_1, h_2 and h_3 — were the ones with the smallest real parts ($\mathrm{Re}(h_3) > \mathrm{Re}(h_2) > \mathrm{Re}(h_1)$), and correspond to azimuthally symmetric guided waves identified as $SW1$, $SW2$ and $SW3$, respectively. Only these guided waves mostly influence the scattering properties of finite-length CNT bundles, as discussed in Sec. V B. We also considered the properties of an azimuthally nonsymmetric guided wave, identified as $NSW1$, which emerges from the solution of Eq. (18) for $\ell = 1$ and the real part of whose wavenumber h is the smallest possible.

The radial dependencies of the magnitude of the z-directed component of the electric field inside the chosen CNT bundle for guided waves $SW1$, $SW2$, $SW3$ and $NSW1$ are shown in Fig. 2. The lines in this figure were obtained from the effective multishell approach of Sec. III, whereas the points were obtained from the many-body technique of Sec. II B. We conclude that the two approaches yielded reasonably close results for the chosen bundle. Such a good coincidence of the results from both approaches was observed only for bundles with closely packed CNTs. For rarified bundles (where the smallest inter-CNT distance exceeds the CNT radius by a factor of 10 or more), the results of both approaches coincide only for the guided wave $SW1$.

As one can be deduced from Fig. 2, the electric field inside the bundle is distributed over the entire cross–section. Outside the bundle, the radial distribution of the electric field is governed by the decreasing modified Bessel function $K_\ell(\sqrt{h^2 - k^2}\rho)$. Thus the electric field is highly localized to the CNT bundle.

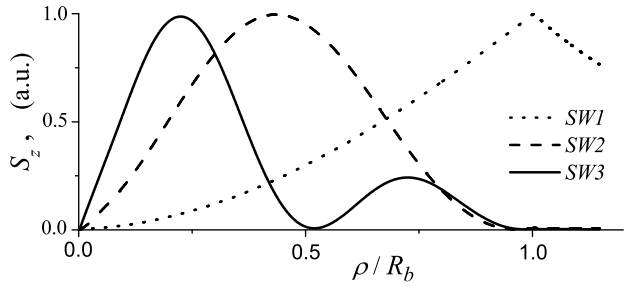

FIG. 3: Radial dependence of the axial component of the time-averaged Pointing vector S_z (in arbitrary units) of the guided waves in the same CNT bundle as in Fig. 2.

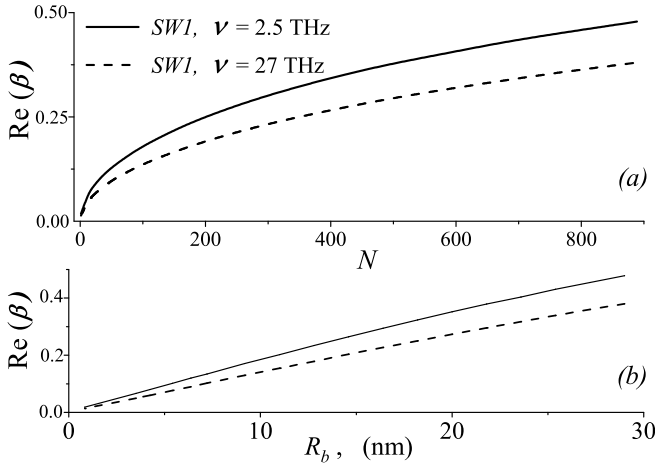

FIG. 4: Dependencies of Re(β) of the guided wave SW1 on (a) the number N of CNTs in the bundle and (b) the bundle radius R_b.

Furthermore, calculations show that the radial field distribution for $SW2$ and $SW3$ can be described adequately by Bessel functions of the first kind $J_0(\kappa_2\rho)$ and $J_0(\kappa_3\rho)$, respectively, where κ_2 and $\kappa_3 > \kappa_2$ are the non-zero minimal roots of the equation $J_1(\kappa R_b) = 0$.

All other results — presented in Fig. 3-7 — were obtained using the effective multishell approach. Figure 3 shows the radial distributions of the axial component of the time-averaged Pointing vector $S_z = c|H_\phi|^2/(8\pi)$ for three azimuthally symmetric guided waves ($SW1$, $SW2$, and $SW3$) inside the CNT bundle ($\rho/R_b < 1$) and in the vicinity of its surface ($\rho/R_b > 1$). As shown in Fig. 3, the axial component of the time-averaged Pointing vector of $SW1$ is maximum near the surface of the bundle, and a large part of the energy of SW1 leaks outside the bundle. In contrast, the power densities of $SW2$ and $SW3$ are mostly concentrated inside the bundle. Thus, the electromagnetic energy and volume electric current density of the guided waves in a CNT bundle are distributed similarly to those of eigenwaves propagating in a macroscopic, lossy, infinitely long wire [22]. Accordingly, guided waves propagating in a CNT bundle with a large number of CNTs cannot be called *surface waves*.

Figure 4(a) contains plots of the real part of the slow-wave coefficient β of the guided wave $SW1$ in the terahertz ($\nu = \omega/2\pi = 2.5$ THz) and infrared ($\nu = 27$ THz) regimes for different numbers of CNTs in the bundle. The coefficient Re(β) increases as much as 26 times with N increasing up to 900. A large N means that the bundle is thick (with $R_b > 25$ nm) and its slow-wave coefficient tends to that of a macroscopic metallic wire. The dependence of Re(β) on the bundle radius is linear up to $R_b = 25$ nm, as may be deduced from Fig. 4(b).

A comparison of Figs. 4(a) and Fig. 5 reveals that Re(β) of $SW1$ is about three, five and nine times more than that of $NSW1$, $SW2$ and $SW3$, respectively. We also found that the solution of the dispersion equation (18) for $NSW1$ does not change in a frequency regime wherein the arguments of Bessel functions $I_\ell(\cdot)$ and $K_\ell(\cdot)$ in Eq. (17) are much smaller than unity, i.e. $\kappa R_b << 1$. This condition holds for realistic CNT bundles over a wide frequency range from the terahertz to the near-infrared regimes [3]. The dependencies of Re(β) on R_b are linear for $SW2$, $SW3$ and $NSW1$ are also linear up to $R_b = 25$ nm (not shown in this paper).

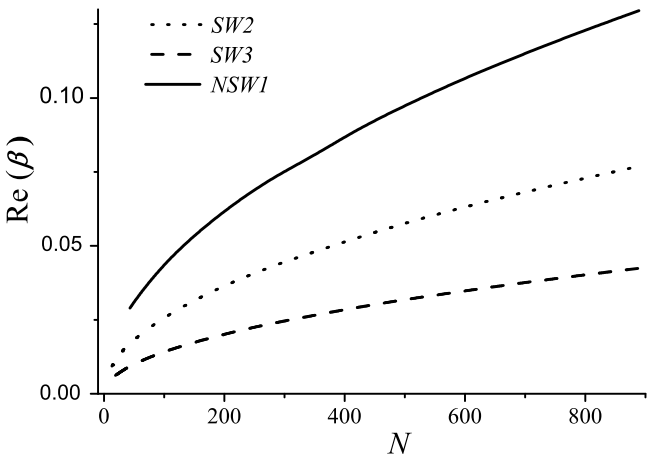

FIG. 5: Dependence of Re(β) on N, for the guided waves SW2, SW2 and NSW1 at $\nu = \omega/2\pi = 27$ THz.

Although not substantiated here by a graph, the value of $-\mathrm{Im}(\beta)/\mathrm{Re}(\beta)$ for the considered guided waves does not depend on N. This implies that the electromagnetic coupling of the CNTs does not influence the attenuation of the guided waves in the bundle. The ratio $-\mathrm{Im}(\beta)/\mathrm{Re}(\beta)$ is approximately equal to 0.32 and 0.034 at $\nu = 2.5$ THz and $\nu = 27$ THz, respectively, for $SW1$.

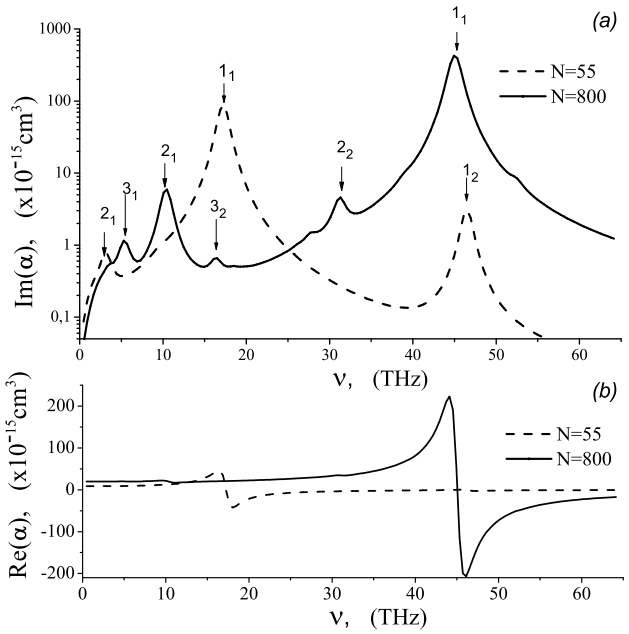

FIG. 6: Frequency dependence of (a) Im(α) and (b) Re(α) of a bundle of CNTs of length $L = 500$ nm. Two values of N were used: 55 and 800. The labels 1, 2 and 3 denote the geometric resonance of the guided waves $SW1$, $SW2$ and $SW3$, respectively. The subscripts on the labels denote the number $\tilde{s}$ of the geometric resonance in Eq. (26).

B. Guided waves in bundles of finite-length CNTs

Let us now move on to almost circular bundles of finite-length CNTs. Fig. 6 demonstrates the frequency dependence of the polarizability scalar α of a bundle of CNTs for two different values N. The labels 1, 2 and 3 in this figure denote the geometric resonance of the guided waves $SW1$, $SW2$ and $SW3$, respectively. Clearly, the polarizability

resonances in this figure occur at frequencies satisfying the condition (26). The location of the first resonance ($\tilde{s} = 1$) of all three guided waves on the frequency axis depends on N. The first geometrical resonance of the $SW1$ is the strongest of the three, and it shifted from the terahertz regime to the mid-infrared regime as N was changed from 1 to 800. The geometrical resonances of $SW2$ and $SW3$ occur at lower frequencies; moreover, they even vanish for small N, because of the strong attenuation of the guided wave at low frequencies (where the condition $\mathrm{Im}(h)/\mathrm{Re}(h) > 1$ holds).

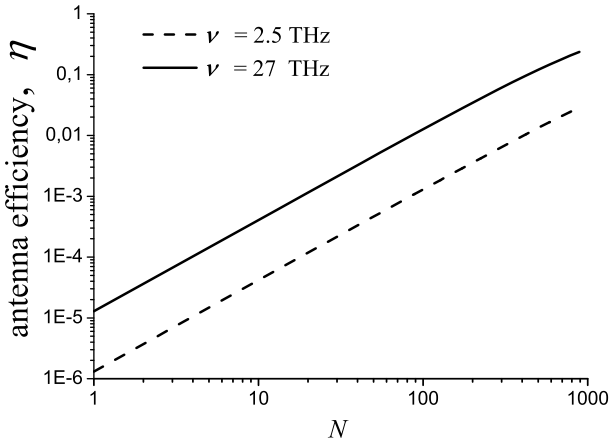

FIG. 7: Dependence of the antenna efficiency η on the number N of CNTs at $\nu = 2.5$ THz (terahertz regime) and $\nu = 27$ THz (infrared regime). The length L was modified to ensure that the condition (26) is satisfied with $\tilde{s} = 1$, for fixed ν.

Similar conclusions could be made for wavelength-dependent resonant effects in the optical regime from measurements on a parallel array of multiwall CNTs [19]. Thus, by varying the bundle radius and the CNT length, one can tune the resonance properties of a CNT bundle functioning as an antenna from the terahertz to the visible regimes. A similar conclusion could be drawn for composite materials containing CNT inclusions [4, 23].

The dependence of the antenna efficiency η on the number N of CNTs in a bundle at two different frequencies $\nu = \omega/2\pi$ is illustrated in Fig. 7. The length L was modified to ensure that a chosen value of ν always corresponds to the first geometrical resonance of SW1 (i.e., the condition (26) is satisfied with $\tilde{s} = 1$). Evidently from Fig. 7, η increases with N and tends to unity for thick bundles ($N > 800$); indeed, $\eta = 0.24$ when $N = 900$ and $\nu = 27$ THz.

VI. CONCLUDING REMARKS

To conclude, an equivalent-multishell approach was proposed for the approximate calculation of the characteristics of electromagnetic guided waves on almost circular, closely packed bundles of parallel, identical, and metallic carbon nanotubes. The CNTs can be either infinitely long or of finite length. The dispersion characteristics of the guided waves with the smallest retardation (i.e., lowest values of $\mathrm{Re}(h)$) where studied for bundles of infinitely long CNTs. The slow-wave coefficients for azimunthally symmetric guided waves were found to increase with the number of metallic CNTs in the bundle, tending for thick bundles to unity, which is characteristic of macroscopic metallic wires. The existence of an azimuthally nonsymmetric guided wave at low frequencies in a bundle of a large number of finite-length CNTs was demonstrated, in contrast to the characteristics of guided-wave propagation in a single CNT.

The polarizability scalar and the antenna efficiency of a bundle of finite-length CNT in the long-wavelength regime were calculated over a wide frequency range spanning the terahertz and the near-infrared regimes. The resonances of different guided waves in CNT bundles caused by edge effects (geometrical resonances) were identified. The antenna efficiency of a CNT bundle at the first antenna resonance can greatly exceed that of a single CNT. Thus, the analysis carried out in this paper forms a basis for the design and development of CNT-bundle antennas and composite materials [24] containing CNT-bundles as inclusions.

ACKNOWLEDGMENTS

The authors are grateful to Dr. G. Ya. Slepyan for helpful discussions. The research of MVS and SAM was partially supported by the NATO Science for Peace program (grant SfP-981051), the State Committee for Science and Technology of Belarus and the INTAS (grant 03-50-4409), the INTAS (grant 05-1000008-7801) and the Belarus

Republican Foundation for Fundamental Research and Russian Foundation for Basic Research (grant F06R-101, F07M-069). The research of AL was partially supported by the Charles Godfrey Binder Professorship Endowment at the Pennsylvania State University.

---

[1] *Selected Papers on Nanotechnology – Theory and Modeling* (F. Wang and A. Lakhtakia, eds), (SPIE Press, Bellingham, WA, 2006).
[2] P. Longe, and S. M. Bose, Phys. Rev. B **48**, 18239 (1993).
[3] G. Ya. Slepyan, S. A. Maksimenko, A. Lakhtakia, O. Yevtushenko, and A. V. Gusakov, Phys. Rev. B **60**, 17136 (1999).
[4] G. Ya. Slepyan, M. V. Shuba, S. A. Maksimenko, and A. Lakhtakia, Phys. Rev. B **73**, 195416 (2006).
[5] G. W. Hanson, IEEE Trans. Antennas Propagat. **53**, 3426 (2005).
[6] P. J. Burke, S. Li, and Z. Yu, IEEE Trans. Nanotechnol. **5**, 314 (2006).
[7] A. A. Maarouf, C. L. Kane, and E. J. Mele, Phys. Rev. B **61**, 11156 (2000)
[8] K. Kempa, Phys. Rev. B **66**, 195406 (2002).
[9] G. Gumbs, and G. R. Aizin, Phys. Rev. B **65**, 195407 (2002).
[10] F. L. Shyu, and M. F. Lin, Phys. Rev. B **62**, 8508 (2000).
[11] M. S. Dresselhaus, G. Dresselhaus, and Ph. Avouris, *Carbon Nanotubes* (Springer, Berlin, 2001).
[12] S. A. Maksimenko, A. A. Khrushchinsky, G. Ya. Slepyan, and P. V. Kibis, J. Nanophoton. **1**, 013505 (2007).
[13] S. A. Maksimenko and G. Ya. Slepyan, in *Electromagnetic Fields in Unconventional Materials and Structures*, edited by O. N. Singh and A. Lakhtakia (Wiley, New York, 2000), pp. 217-255.
[14] M. F. Lin, D. S. Chuu, C. S. Huang, Y. K. Lin, and K. W.-K. Shung, Phys. Rev. B **53**, 15493 (1996).
[15] M. A. Abramovitz, and I. A. Stegun, *Handbook of Mathematical Functions* (Dover Press, New York, 1972).
[16] J. Hao, and G. W. Hanson, Phys. Rev. B **74**, 035119 (2006).
[17] J. Hao, and G. W. Hanson, Phys. Rev. B **75**, 165416 (2007).
[18] L. A. Weinstein, *The Theory of Diffraction and the Factorization Method* (Golem, New York, 1969).
[19] Y. Wang, K. Kempa, B. Kimball, J. B. Carlson, G. Benham, W. Z. Li, T. Kempa, J. Rybczynski, A. Herczynski, and Z. F. Ren, Appl. Phys. Lett. **85**, 2607 (2004).
[20] K. Kempa, J. Rybczynski, Z. Huang, K. Gregorczyk, A. Vidan, B. Kimball, J. Carlson, G. Benham, Y. Wang, A. Herczynski, and Z. Ren, Adv. Mater. **19**, 421 (2007).
[21] Z. Yu, C. Rutherglen, and P. J. Burke, Appl. Phys. Lett. **88**, 233115 (2006).
[22] A. Sommerfeld, *Electrodynamics* (Academic, New York, 1952).
[23] A. Lakhtakia, G. Ya. Slepyan, S. A. Maksimenko, O. M. Yevtushenko, A. V. Gusakov, Carbon **36**, 1833 (1998).
[24] *Selected Papers on Linear Optical Composite Materials* (A. Lakhtakia, ed), (SPIE Press, Bellingham, WA, 1996).